MUON ABSOLUTE LIFETIME EVALUATION FOR NEUTRINO NUCLEAR RESPONSE USING RUTHENIUM OXIDE THIN FILMS TARGET

NIK NOOR AIEN BINTI MOHAMED ABDUL GHANI

UNIVERSITI TEKNOLOGI MALAYSIA

MUON ABSOLUTE LIFETIME EVALUATION FOR NEUTRINO NUCLEAR RESPONSE USING RUTHENIUM OXIDE THIN FILMS TARGET

NIK NOOR AIEN BINTI MOHAMED ABDUL GHANI

A thesis submitted in fulfilment of the
requirements for the award of the degree of
Doctor of Philosophy

Faculty of Science
Universiti Teknologi Malaysia

MAY 2022

DEDICATION

I dedicate my dissertation work wholeheartedly to my family and many friends. A special thanks to my loving parents, Che Siti Nor and the memory of my late father, Allahyarham Drs. Hj Mohamed Abdul Ghani bin Haji Ibrahim (A.M.N) who had passed away on Friday / 10 May 2019 / 5 Ramadan 1440.

They have been a source of inspiration and strength through my thick and thin throughout the process. I will always appreciate those words of encouragement, moral and spiritual support.

ACKNOWLEDGEMENT

Thanks to Allah for giving me the strength to complete this study after fulfilling various obstacles. Thanks to my father who drove my life journey, my mother who gave her words of passion, husband and daughter who have always been with me when it was hard and depleted throughout this PhD journey. Not forgetting my family-in-law for their prayed and supported throughout this journey. Millions of thanks to my supervisor, Dr Izyan Hazwani binti Hashim, for helping, and encouraging throughout the entire process of this thesis. The bad ones are from me, and the good ones all come from Allah s.w.t

ABSTRACT

Muon absolute lifetime is a measured lifetime of the trapped muons particle in a target nucleus by the ordinary muon capture (OMC) process. OMC is the probe for neutrino and astro-antineutrino nuclear response (NNR) that is relevant to double beta decay (DBD). The total OMC rates with relative capture strength can be used to determine the muon matrix element. The OMC rates for several DBD candidates reported in the theoretical and experimental studies show the quenching effect in the experimental OMC rate values which lead to high discrepancies in the DBD nuclear matrix element (NME). Ruthenium (Ru) is one of the DBD nucleus that is important for neutrino studies in nuclear and astroparticle physics using muon capture reactions. The present experimental work is the first measurement on Ru for NNR study by OMC experiment. Muon irradiation will transform the ${}^{A}_{Z}X$ nucleus to ${}_{Z-1}^{A}Y$ nucleus via the exchange of weak bosons. A new synthesis method of Ru thin film target is developed in the present study to fulfil the muon irradiation criteria. A ruthenium oxide (RuO_2) thin film target is carefully synthesised using normal evaporation method. Poly (vinyl alcohol) (PVA) and RuO_2 powder are mixed with H_2O separately to form two solutions. The thin film is analysed using several instruments to investigate the target's characteristics. Field emission scanning electron microscope with energy dispersive X-ray (FESEM-EDX) is used to determine the thickness, uniformity, morphology and elemental identification of the thin film. Inductively coupled plasma-triple quadrupole mass spectrometer (ICPMS) and inductively coupled plasma-optical emission spectrometer (ICPOES) are essential for analyses as they can confirm the concentration of natural contamination (${}^{40}K$, ${}^{238}U$, ${}^{232}Th$) in the thin film. X-ray diffraction (XRD), Raman, and Fourier transform infrared with attenuated total reflection (FTIR-ATR) are used for extended analyses to confirm the hydration phenomena observed in FESEM-EDX. The target was irradiated using negative muons at MuSIC facility at Osaka University, Japan. The muon to electron decay and radioisotope (RI) gamma-rays are processed and recorded by scintillation detectors and high purity germanium (HPGe) detectors. The new synthesis method is suitable for multiple productions of thin film targets. The final thickness for the OMC experiment can be controlled as obtained from some hydration evidence of RuO_2 thin film. The muon absolute lifetime of Ru obtained in this experiment is 132.7 ns, equivalent to 7.54×10^6 s $^{-1}$ total muon capture rate. Present observations confirm slight quenching to the effective axial coupling constant (g_A^{eff}) parameter at about 33% error. The experimental OMC rates of Ru can deduce the absolute neutrino and antineutrino nuclear responses for DBD and neutrino properties of astrophysics origin.

ABSTRAK

Jangka hayat mutlak muon adalah ukuran jangka hayat zarah muon yang terperangkap dalam nukleus sasaran melalui proses penangkapan muon biasa (OMC). OMC adalah penduga untuk sambutan nuklear neutrino dan astro-antineutrino (NNR) yang berkait dengan pereputan beta berganda (DBD). Jumlah kadar OMC dengan kekuatan tangkapan relatif boleh digunakan untuk menentukan elemen matriks muon. Kadar OMC untuk beberapa calon DBD yang dilaporkan dalam kajian teori dan eksperimen menunjukkan kesan pelindapkejutan dalam nilai kadar OMC eksperimen yang membawa kepada percanggahan tinggi dalam elemen matriks nuklear (NME) DBD. Ruthenium (Ru) adalah salah satu nukleus DBD yang penting untuk kajian neutrino dalam fizik nuklear dan astropartikel menggunakan tindak balas tangkapan muon. Kajian eksperimen ini adalah pengukuran pertama pada Ru untuk kajian NNR menggunakan eksperimen OMC. Sinaran muon akan mengubah nukleus ${}^{A}_{Z}X$ kepada nukleus ${}^{A}_{Z-1}Y$ melalui pertukaran boson lemah. Kaedah sintesis baharu sasaran filem tipis Ru telah dibangunkan dalam kajian ini untuk memenuhi kriteria penyinaran muon. Sasaran filem tipis ruthenium oksida (RuO_2) disintesis dengan teliti menggunakan kaedah penyejatan biasa. Poli (vinil alkohol) (PVA) dan serbuk RuO_2 dicampur dengan H_2O secara berasingan untuk membentuk dua campuran. Filem tipis dianalisa menggunakan beberapa instrumen untuk mengkaji ciri-ciri sasaran. Mikroskop elektron pengimbasan pancaran medan dengan sebaran tenaga sinar-X (FESEM-EDX) digunakan untuk menentukan ketebalan, keseragaman, morfologi dan penentuan unsur filem tipis. Spektrometer jisim plasma berganding aruhan – catur kutub empat tigaan (ICPMS) dan spektrofotometer pancaran optik – plasma berganding aruhan (ICPOES) adalah penting untuk analisis kerana ia dapat mengesahkan kepekatan pencemaran semulajadi (^{40}K, ^{238}U, ^{232}Th) dalam filem tipis. Belauan sinar-X (XRD), Raman, dan spektroskopi inframerah transformasi Fourier dengan pengecilan jumlah pantulan (FTIR-ATR) digunakan untuk analisis lanjutan untuk mengesahkan fenomena penghidratan yang diperhatikan dalam FESEM-EDX. Sasaran itu disinari menggunakan muon negatif di MuSIC, Universiti Osaka, Jepun. Pereputan muon kepada elektron dan radioisotop (RI) sinar gama diproses dan direkodkan oleh pengesan sintilasi dan pengesan germanium berkepekatan tinggi (HPGe). Kaedah sintesis baharu ini sesuai untuk penghasilan sasaran filem tipis secara berulang. Ketebalan muktamad untuk experimen OMC boleh dikawal seperti yang diperolehi daripada bukti penghidratan filem tipis RuO_2. Jangka hayat mutlak muon Ru yang diperolehi dalam eksperimen ini adalah 132.7 ns, bersamaan dengan $7.54 \times 10^6\ s^{-1}$ jumlah kadar tangkapan muon. Cerapan mengesahkan sedikit pelindapkejutan ke atas parameter pemalar gandingan paksi berkesan (g_A^{eff}) kira-kira 33% ralat. Kadar OMC Ru eksperimen dapat mendeduksi sambutan nuklear neutrino dan antineutrino mutlak untuk sifat DBD dan neutrino untuk asal-usul astrofizik.

TABLE OF CONTENTS

LIST OF TABLES

LIST OF FIGURES

LIST OF ABBREVIATIONS

μSR	-	Muon spin rotation
ADC	-	Analogue digital converter
Al	-	Aluminium
Co	-	Cobalt
DAQ	-	Data acquisition
DBD	-	Double beta decay
EC	-	Electron capture
EDX	-	Energy dispersive X-ray
Eu	-	Europium
EWSR	-	Energy weighted sum rule
FESEM	-	Field emission scanning electron microscope
FTIR-ATR	-	Fourier transform infrared with attenuated total reflection
FWHM	-	Full width of half maximum
GUI	-	Graphical user interface
GP	-	Goulard Primakoff
HCL	-	Hydrocloric acid
HNO_3	-	Nitric acid
HPGe	-	High purity germanium
IBD	-	Inverse beta decay
ICPMS	-	Inductive coupled plasma quadrupole mass spectrometer
ICPOES	-	Inductive coupled plasma optical emission spectrometer
ISM	-	Interactive shell model
JPARC	-	Japan proton accelerator research complex
K	-	Pottasium
Mo	-	Molybdenum
MuSIC	-	Muon science innovative channel

MUSE	-	Muon science establishment
^{Nat}Ru	-	Natural ruthenium
NAA	-	Neutron activation analysis
NEWSR	-	Non energy weighted sum rule
NME	-	Nuclear matrix element
NNR	-	Neutrino nuclear response
NIP	-	Nuclear isotope production
OMC	-	Ordinary muon capture
ppb	-	part per billion
PVA	-	Poly (vinyl alcohol)
PNEM	-	Proton neutron emission model
QRPA	-	Quasiparticle random phase approximation
RCNP	-	Research Centre for Nuclear Physics
RI	-	Radioactive isotope
RMC	-	Radiative muon capture
RTV	-	Room temperature vulcanising
Ru	-	Ruthenium
RuO_2	-	Ruthenium oxide
SμS-PSI	-	Swiss muon source at Paul Scherrer Institute
SBD	-	Single beta decay
SCA	-	Single-channel analyser
SM	-	Standard model
Th	-	Thorium
TC	-	Technetium
TDC	-	Time digital converter
TPC	-	Time projection chamber
U	-	Uranium
XRD	-	X-ray diffraction
ε	-	Efficiency

LIST OF SYMBOLS

μ^-	-	Negative muon
μ^+	-	Positive muon
J_π	-	Spin state
s	-	Second
e	-	Electron
τ	-	Tau
υ	-	Neutrino
υ_e	-	Electron neutrino
υ_μ	-	Muon neutrino
υ_τ	-	Tau neutrino
A	-	Atomic weight
Z	-	Atomic number
Z_{eff}	-	Effective atomic mass
γ	-	Gamma
Λ_t	-	Total capture rate
Λ_c	-	Partial capture rate
d	-	Decay rate
Q	-	Huff factor
β^+	-	Beta plus
β^-	-	Beta minus
$\beta\beta$	-	Double beta
n	-	Neutron
α	-	Alpha
X	-	Muon capture rates
N_a	-	Avogadro's number
r_e	-	Electron radius

υ_e	-	Electron neutrino
$-\frac{dE}{dX}$	-	Stopping power
m_e	-	Electron mass
I	-	Mean excitation potential
ρ	-	Density
z	-	Charge of incident particle
c	-	Speed of light
γ	-	Lorentz factor
δ	-	Density correction
C	-	Shell correction
$h\upsilon_p$	-	Plasma frequency
N_e	-	Electron density
W_{max}	-	Maximum energy transfer
M	-	Mass of incident particle
λ	-	Incident X-rays
T	-	Thickness
t	-	Thickness density
I	-	Intensity
N_μ	-	Number of muon
Br	-	Branching ratio
$Y(\gamma)$	-	Gamma yield
Ω	-	solid angle
W	-	Boson
g_A^{eff}	-	Effective axial coupling
g_{pp}	-	Particle-particle interaction
g_A	-	Axial-vector coupling
g_p	-	Spin-isospin
η_c	-	muon capture probability
η_s	-	muon stopping probability

LIST OF APPENDICES

APPENDIX	TITLE	PAGE

CHAPTER 1

INTRODUCTION

1.1 Research Background

In the standard model (SM), a muon (μ) is a kind of lepton with a mass of 105 MeV/c^2 that interacts via weak boson by exchange with its associated neutrinos (υ_μ). On average, from positive muon (μ^+) and negative muon (μ^-) decays, the reported lifetime is 2.2μs [1]. The decay of μ^+ is mostly contributed by free muon decay, but μ^- muon decay is material-dependent. Identifying the lifetime is difficult for μ^- due to the presence of matter and considering the stoppage and disappearance of μ^- in the matter that may affect muon capture rates in the nuclei. Due to the interaction with matter, the lifetime of μ^- is much smaller as the A's mass number increases.

The study of neutrino nuclear response (NNR) is useful to investigate the fundamental properties of neutrinos that have come to light over decades, such as the nature of a neutrino: Majorana or Dirac, mass hierarchy or absolute mass, the lepton sector-CP phase, solar neutrino source and the fluxes, supernova neutrino intensities and nucleosynthesis [2]. Many experimental works have been done to investigate neutrinos' properties via nuclear reaction, such as single beta decay (SBD) or electron capture (EC), inverse beta decay (IBD) and double beta decay (DBD). A review of these experimental works has been summarised in the references [3]. Physicists have used these processes to extract the neutrino mass average (M_{ave}) provided by the nuclear matrix elements (NME). NME includes the nucleonic and non-nucleonic correlations effects from the nuclear structure.

DBD is a rare nuclear transition. The slowest process in nature happens in the area of weak interaction in nuclei. It comes in two modes, which are neutrinoless $\beta\beta$ decay ($0\upsilon\beta\beta$) and two neutrinos $\beta\beta$ decay ($2\upsilon\beta\beta$). NNR in SBD and IBD cases refers to the excitation energy range of the remaining nucleus after neutrino emission. The square root of NME ($M_{0\upsilon}$ and $M_{2\upsilon}$) in DBD indicates the parent's transition to the daughter nucleus through the multilevel intermediate state (J^{π} spin state). Investigating neutrino properties beyond the standard model has been an interest among scientists in experimental and theoretical fields. However, the feasible method to investigate the Majorana nature of neutrinos is by $0\upsilon\beta\beta$ decay [4]. $0\upsilon\beta\beta$ is a lepton number violating mode where the neutrino only occurs as a virtual particle, which is not allowed in the standard model.

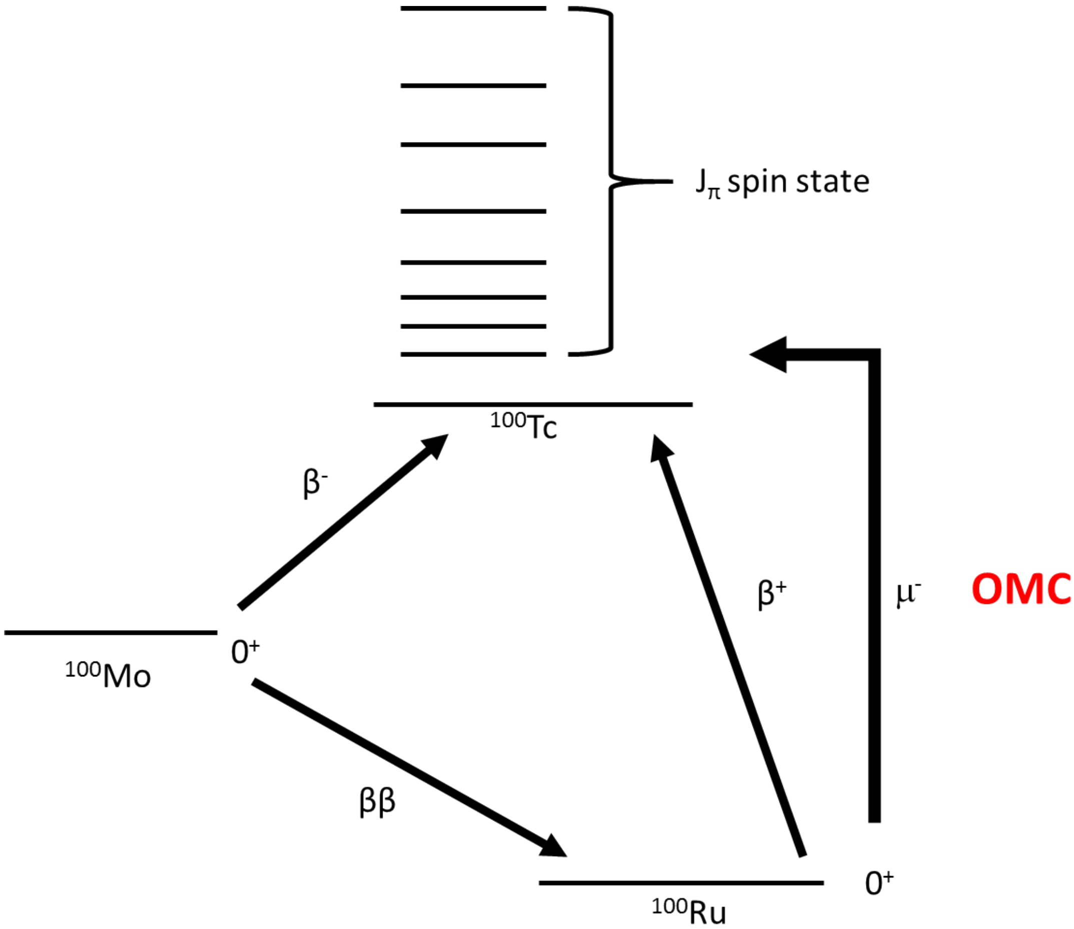

Figure 1.1: $\beta\beta$ decay of ^{100}Mo to ^{100}Ru through intermediate nuclei (^{100}Tc). The ordinary muon capture (OMC) on ^{100}Ru can access the β^{+} side of $\beta\beta$ decay.

Ordinary muon capture (OMC) can extract the single M (β^{+}) matrix by accessing the high J^{π} spin state of nuclei that are similar to the $0\upsilon\beta\beta$ process [5]. Figure 1.1 shows the OMC reaction can be a probe to study the intermediate nuclei of ^{100}Tc from the DBD of ^{100}Mo to ^{100}Ru from the β^{+} side. Furthermore, the muon capture may excite the target nuclei up to 100 MeV excitation energy (equivalent to J^{π} states = ± 6)

more than other probes. One can obtain the muon capture strength by measuring the delayed γ-rays after OMC and comparing the results with the proton-neutron emission model (PNEM) [6]. The theoretical pn-QRPA and QRPA can be used to reproduce the experimental μ capture strength and evaluate the OMC rate and other nuclear parameters [7, 8]

From Eq. 1.1, the OMC rate from the OMC experiment can be determined by direct measurement of muon absolute lifetime [9] or partial μ capture rates from bound states [4]. The relations between muon absolute lifetime, total capture rate and partial capture rate can be expressed by;

$$\frac{1}{\tau} = \Lambda_t = \Lambda_c + Q\Lambda_d \tag{1.1}$$

where muon absolute lifetime (τ) is the inverse of the total muon capture rate, Λ_t, that is also the sum product of partial capture rate, Λ_c, and decay rate, Λ_d. The Huff factor, Q, is included as a corrector for the unbound electron in the shell. Note that Q is approximately 1 for light nuclei, which is much smaller for the medium-heavy nuclei.

The OMC rate prediction on ^{100}Ru using the pn-QRPA and QRPA model shows a large difference value [7, 8]. Thus, the comparison with the experimental OMC rate is needed to evaluate the $0\upsilon\beta\beta$ decay of NME accuracy. Using the material with natural isotopic abundance of ruthenium ($^{\mathrm{Nat}}$Ru) in the form of RuO_2 powder would act as a control system to the ^{100}Ru data later.

In the muon capture reaction, a negative muon μ^- is stopped in the proton in the nucleus and transformed into a neutron by reducing one proton number with the emission of the muon neutrino, as shown in Eq. 1.2 and Eq. 1.3.

$$\mu^- +_1^1 p \longrightarrow_0^1 n + \upsilon_\mu \tag{1.2}$$

$$\mu^- +_Z^A X \longrightarrow_{Z-1}^A X + \upsilon_\mu \tag{1.3}$$

Suppose the final nucleus is in the excited states. In that case, it will release RI gamma rays possessing the same A and Z-1 [10, 11]. The experimental statistics of both RI gamma rays and electron decay can be enhanced using suitable target thickness.

Reviewing the previous OMC experiment, several targets with different target designs have been used, such as gas, liquid, bulk, powder, and thin film. Since the $\beta\beta$ decay nuclei occur in heavy and medium-heavy nuclei, the target must be thin; up toμm to mm [12]. A film type target thickness can be adjusted based on the desired muon beam intensity. In addition, a target with less contaminants and uniformly distributed increases the sensitivity of gamma detections [13]. These requirements are necessary to extract more experimental events in the OMC experiment and reduce the energy loss in the target [14, 15, 16].

The preparation of the thin film target used the normal evaporation process, which is the simplest way to fabricate samples of any metal or non-metals and enriched or natural isotopes. Moreover, the physical, structural and elemental analyses presented are helpful to get more information about the characteristics of the target for the muon capture experiment.

1.2 Problem Statement

This study covers the measurement of muon absolute lifetime of ruthenium targets through an OMC experiment to investigate the neutrino properties in NNR for DBD study. The OMC rate can be measured or calculated from the muon absolute lifetime. Therefore, the researchers compared OMC rates from several DBD nuclei to investigate the problem, including the quenching effect from the NME of DBD.

From previous works, the theoretical OMC rates using pn-QRPA calculated by Jokiniemi and Suhonen [7] show a greater value than the experimental rate reported by Suzuki and Measday [9] and Zinatulina [4] and also than using Primakoff's equation prediction [17]. Meanwhile, using the theoretical QRPA model, Simkovic [8] had obtained a value of OMC rate lower than that in the experiment by Suzuki and Daniya and predicted by Goulard Primakoff's (GP) equation. The differences in OMC rates from both theoretical calculations are due to the assumption of both models' nucleonic and non-nucleonic nuclear structure effects.

Suzuki and Measday reported the OMC rate for nuclei with Z=1 until Z=94 by showing an increasing pattern as a function of Z [9]. On the other hand, Primakoff obtained the OMC rates from the subtraction of the Pauli Exclusion Principle in the nuclear environment from the OMC rates of hydrogen [17]. He also provided the extension to the Pauli Exclusion Principle for heavy nuclei. The partial capture rates for nuclei in the range of $36 \leq Z \leq 62$ were experimentally observed by Zinatulina [4]. Theoretically, Jokiniemi and Suhonen compare the relative capture strength obtained from the experiment by Hashim [6] and deduced the absolute capture strength using suitable axial-vector coupling parameters.

An enriched or high purity target helps minimise other beta decay contributions during the measurement and analysis of the RI production experiments [10, 18]. However, there are possible contaminations from beta decay in Suzuki muon absolute lifetime measurements due to the use of self-supporting powder-type targets [9]. This problem leads to the OMC target being prepared to suit the OMC experiment and enhance the OMC outcome. The value of the theoretical muon capture rate from Jokiniemi shows a large quenching of the structural parameter g_A^{eff} that is in accordance with the earlier study of beta decay [7]. Hence, the approximation of muon disappearance rate from experimental work, which corresponds to the inverse of electron decay lifetime, would affect the differences.

The targets used in the previous OMC experiment were either gas, liquid or bulk, including powder targets. The gas and liquid targets require a particular container to contain them at a specific pressure [19, 20]. In contrast, they are the preferred type for bulk targets due to their handling credibility and lack of requirement for special preparation [21]. Powder targets are packed into a flat container made of polyethylene film to hold the powder during the experiment [4]. Thin film is another good option for a target compared to the powder form since it is uniformly distributed and easy to handle [14].

1.3 Research Objectives

The research objectives are listed as follows:

1. To fabricate the RuO_2 thin-film target for OMC experiments by the normal evaporation method.
2. To characterise RuO_2 thin-film targets (hydrate and anhydrous) in terms of morphology, elemental and structural properties.
3. To evaluate the muonic X-ray and gamma-ray for total muons stopped in target and radioisotope production after muon capture.
4. To determine the muon absolute lifetime of ruthenium.

1.4 Scope of Study

The present study of the OMC rate of ruthenium, as well as the fabrication and characterisation of RuO_2 thin film is included as preliminary work to measure the muon absolute lifetime for NNR. The film preparation adopts a new synthesis process from the normal evaporation technique. Here, two types of RuO_2 thin film, hydrate and anhydrous, are fabricated where the morphology, elemental and structural analyses are compared. FESEM-EDX checks the thin film's thickness and uniformity distributions. ICPMS and ICP-OES observe and identify elemental impurities. Meanwhile, the observed hydration in the hydrate thin film is further examined by XRD, FTIR, and Raman analysis. Several thin film pieces are stacked into 260 mg/cm^2 thickness and irradiated by high intense muons from the MuSIC beamline at 45 MeV/c^2 for 1 hour and 30 minutes. Three scintillation counters act as a trigger counter for the muon stopping signal to differentiate the data recorded for muonic X-rays, RI gamma rays, and electron decay. The measurements and the analyses are reported on and discussed.

1.5 Significance of Study

The outcome of the present work is important for $0\upsilon\beta\beta$ studies since the fundamental properties of neutrinos have yet to be concluded. The extraction of the properties of neutrinos from $0\upsilon\beta\beta$ DBD experiments is important in providing the information on neutrino effective mass and the nature of massive neutrinos at the β^+ side of NME DBD. Furthermore, the finding of neutrino mass and Majorana neutrino could help the comprehension of physics beyond the standard model (SM) where for $0\upsilon\beta\beta$, the neutrino only occurs as a virtual particle which is not allowed in SM. The OMC process can provide the single matrix elements of β^+. Hence, the muon absolute lifetime measurement from OMC experiments can provide information of muon capture strength distribution that later will contribute to the theoretical evaluation in QRPA and pn-QRPA for DBD.

1.6 Thesis Outline

This thesis contains five chapters. Chapter 1 includes the research background, problem statement, four objectives, scope and the significance of the study. Chapter 2 is the literature review, where the discussion of previous data is presented. This chapter explains in detail the current research based on the problem statement, including the summary of comparative literature. Chapter 3 presents the methodology of the project, including the explanation of the experimental technique and introduction to the new synthesis process that produces the RuO_2 thin film target. This chapter is divided into three parts: the estimation method for thin film thickness, synthesis process of the thin film, analysis of the thin film's properties using several instruments, the experiment of the muon irradiation process and the method of analysis of muon irradiation experiments, including the efficiency and resolution of the detector used. Chapter 4 presents the results of the muon absolute lifetime experiment in conjunction with the muon capture rate. The outcome analysis of the OMC process is analysed for muonic X-ray and gamma-ray identification. This chapter includes the comparison of two thin films that were used in the current study, which are hydrate and anhydrous.

Chapter 5 explains the conclusion of the current study and the recommendations for future studies.

REFERENCES

1. Qian, T. *A Precise Measurement of Muon Lifetime at Brookhaven National Laboratory Muon Storage Ring*. Ph.D. Thesis. University of Minnesota. 2006.

2. Ejiri, H., Suhonen, J. and Zuber, K. Neutrino–Nuclear Responses for Astro-neutrinos, Single Beta Decays and Double Beta Decays. *Physics Reports*, 2019. ISSN 03701573.

3. Ejiri, H. Experimental Studies of Neutrino Nuclear Responses and Nuclear Structures for Neutrino Nuclear Physics. *Journal of Physics: Conference Series*. IOP Publishing. 2018, vol. 1056. 012019.

4. Zinatulina, D., Brudanin, V., Egorov, V., Petitjean, C., Shirchenko, M., Suhonen, J. and Yutlandov, I. Ordinary Muon Capture Studies for the Matrix Elements in $\beta\beta$ Decay. *Physical Review C*, 2019. 99(2): 024327.

5. Kortelainen, M. and Suhonen, J. Ordinary Muon Capture as a Probe of Virtual Transitions of $\beta\beta$ Decay. *EPL (Europhysics Letters)*, 2002. 58(5): 666.

6. Hashim, I., Ejiri, H., Othman, F., Ibrahim, F., Soberi, F., Ghani, N., Shima, T., Sato, A. and Ninomiya, K. Nuclear Isotope Production by Ordinary Muon Capture Reaction. *Nuclear Instruments and Methods in Physics Research Section A: Accelerators, Spectrometers, Detectors and Associated Equipment*, 2020: 163749.

7. Jokiniemi, L., Suhonen, J., Ejiri, H. and Hashim, I. Pinning Down the Strength Function for Ordinary Muon Capture on ^{100}Mo. *Physics Letters B*, 2019. 794: 143–147.

8. Šimkovic, F., Dvornickỳ, R. and Vogel, P. Muon capture rates: Evaluation within the quasiparticle random phase approximation. *Physical Review C*, 2020. 102(3): 034301.

9. Suzuki, T., Measday, D. F. and Roalsvig, J. Total Nuclear Capture Rates for Negative Muons. *Physical Review C*, 1987. 35(6): 2212.

10. Ejiri, H., H. Hashim, I., Hino, Y., Kuno, Y., Matsumoto, Y., Ninomiya, K., Sakamoto, H., Sato, A., Shima, T., Shinohara, A. *et al.* Nuclear γ Rays from

Stopped Muon Capture Reactions for Nuclear Isotope Detection. *Journal of the Physical Society of Japan*, 2013. 82(4): 044202.

11. Hashim, I., Ejiri, H., Shima, T., Takahisa, K., Sato, A., Kuno, Y., Ninomiya, K., Kawamura, N. and Miyake, Y. Muon Capture Reaction on ^{100}Mo to Study the Nuclear Response for Double-β Decay and Neutrinos of Astrophysics Origin. *Physical Review C*, 2018. 97(1): 014617.

12. Kortelainen, M. and Suhonen, J. Microscopic study of muon-capture transitions in nuclei involved in double-beta-decay processes. *Nuclear Physics A*, 2003. 713(3-4): 501–521.

13. Ejiri, H., Shima, T., Miyamoto, S., Horikawa, K., Kitagawa, Y., Asano, Y., Date, S. and Ohashi, Y. Resonant photonuclear reactions for isotope transmutation. *Journal of the Physical Society of Japan*, 2011. 80(9): 094202.

14. Kudomi, N., Shima, T., Ejiri, H., Tanaka, J. and Watanabe, T. Preparation of Large and Thin Source Films for Studying Nuclear Rare Decays. *Nuclear Instruments and Methods in Physics Research Section A: Accelerators, Spectrometers, Detectors and Associated Equipment*, 1992. 322(1): 53–56.

15. Sugai, I., Aratani, M., Yanokura, M., Kato, H. and Watanabe, T. A New Technique for the Preparation of very High Purity Enriched ^{100}Mo Disk targets. *Nuclear Instruments and Methods in Physics Research Section A: Accelerators, Spectrometers, Detectors and Associated Equipment*, 1993. 329(1-2): 46–49.

16. Parker, W., De Croes, M. and Sevier Jr, K. Some Methods in the Preparation of Radio-active Materials for use in Beta-spectroscopy. *Nuclear Instruments and Methods*, 1960. 7(1): 22–36.

17. Primakoff, H. Theory of Muon Capture. *Reviews of Modern Physics*, 1959. 31(3): 802.

18. Ejiri, H. and Shima, T. Resonant Photonuclear Isotope Detection using Medium-energy Photon Beam. *Physical Review Special Topics-Accelerators and Beams*, 2012. 15(2): 024701.

19. Shitov, Y., Egorov, V., Briançon, C., Brudanin, V., Deutsch, J., Filipova, T., Petitjean, C., Prieels, R., Siiskonen, T., Suhonen, J. *et al.* Doppler-

broadening of Gamma Rays following Muon Capture: Search for Scalar Coupling. *Nuclear Physics A*, 2002. 699(3-4): 917–935.

20. Bardin, G., Duclos, J., Magnon, A., Martino, J., Richter, A., Zavattini, E., Bertin, A., Piccinini, M., Vitale, A. and Measday, D. A Novel Measurement of the Muon Capture Rate in Liquid Hydrogen by the Lifetime Technique. *Nuclear Physics A*, 1981. 352(3): 365–378.

21. Zinatulina, D., Gromov, K., Brudanin, V., Briançon, C., Egorov, V., Klinskih, A., Petitjean, C., Shirchenko, M. and Yyutlandov, I. Muon Capture in Ti, Se, Kr, Cd and Sm. *AIP Conference Proceedings*. AIP. 2007, vol. 942. 91–95.

22. Hashim, I. H. B. *A Study of Weak Nuclear Response by Nuclear Muon Capture*. Ph.D. Thesis. Osaka University. 2014.

23. Suhonen, J. and Civitarese, O. Weak-interaction and Nuclear-structure Aspects of Nuclear Double Beta Decay. *Physics Reports*, 1998. 300(3-4): 123–214.

24. Kortelainen, M. and Suhonen, J. Analysis of the $2\nu\beta\beta$ Decay and Muon-capture Reactions for the Mass A= 46 and A= 48 Nuclei using the Nuclear Shell Model. *Physics of Atomic Nuclei*, 2004. 67(6): 1202–1205.

25. Horoi, M. and Brown, B. Shell-Model Analysis of the Xe 136 Double Beta Decay Nuclear Matrix Elements. *Physical Review Letters*, 2013. 110(22): 222502.

26. Haxton, W. and Stephenson Jr, G. Double Beta Decay. *Progress in Particle and Nuclear Physics*, 1984. 12: 409–479.

27. Ford, K. W. and Wills, J. G. Muonic Atoms and the Radial Shape of the Nuclear Charge Distribution. *Physical Review*, 1969. 185(4): 1429.

28. Tran, N. H. *A study of Proton Emission Following Nuclear Muon Capture for the COMET experiment*. Ph.D. Thesis. Osaka University. 2014.

29. Goulard, B. and Primakoff, H. Nuclear Muon-capture Sum Rules and Mean Nuclear Excitation Energies. *Physical Review C*, 1974. 10(5): 2034.

30. Measday, D. F. The Nuclear Physics of Muon Capture. *Physics Reports*, 2001. 354(4-5): 243–409.

31. Hänscheid, H., David, P., Konijn, J., Krogulski, T., de Laat, C., Mayer-Kuckuk, T., Petitjean, C., Polikanov, S., Reist, H., Risse, F. *et al.* Muon Capture Rates in ^{233} U, ^{234} U, ^{235} U, ^{236} U, ^{238} U, and ^{237} Np. *Zeitschrift für Physik A Atomic Nuclei*, 1990. 335(1): 1–8.

32. Renga, F. Experimental Searches for Muon Decays Beyond the Standard Model. *Reviews in Physics*, 2019. 4: 100029.

33. Van Ritbergen, T. and Stuart, R. G. On the Precise Determination of the Fermi Coupling Constant from the Muon Lifetime. *Nuclear Physics B*, 2000. 564(3): 343 – 390.

34. Meyer, S., Anderson, E., Bleser, E., Lederman, I., Rosen, J., Rothberg, J. and Wang, I.-T. Precision Lifetime Measurements on Positive and Negative Muons. *Physical Review*, 1963. 132(6): 2693.

35. Klinskikh, A., Brianson, S., Brudanin, V., Egorov, V., Petitjean, C. and Shirchenko, M. Muon Capture in Ar. The Muon Lifetime and Yields of Cl Isotopes. *Bulletin of the Russian Academy of Sciences: Physics*, 2008. 72(6): 735–736.

36. Gninenko, S. Muon Capture Rates from Precision Measurements of the Muon Disappearance. *arXiv preprint arXiv:1302.6398*, 2013.

37. Andreev, V., Banks, T., Carey, R., Case, T., Clayton, S., Crowe, K., Deutsch, J., Egger, J., Freedman, S., Ganzha, V. *et al.* Measurement of Muon Capture on the Proton to 1% Precision and Determination of the Pseudoscalar Coupling g P. *Physical review letters*, 2013. 110(1): 012504.

38. Andreev, V., Banks, T., Case, T., Chitwood, D., Clayton, S., Crowe, K., Deutsch, J., Egger, J., Freedman, S., Ganzha, V. *et al.* Measurement of the Muon Capture Rate in Hydrogen Gas and Determination of the Proton's Pseudoscalar Coupling g P. *Physical Review Letters*, 2007. 99(3): 032002.

39. Daniel, H. Application of X rays from Negative Muons. *Nuclear Instruments and Methods in Physics Research Section B: Beam Interactions with Materials and Atoms*, 1984. 3(1-3): 65–70.

40. Kubo, M., Moriyama, H., Tsuruoka, Y., Sakamoto, S., Koseto, E., Saito, T. and Nishiyama, K. Non-destructive Elemental Depth-profiling with Muonic

X-rays. *Journal of Radioanalytical and Nuclear Chemistry*, 2008. 278(3): 777–781.

41. Ninomiya, K., Nagatomo, T., Kubo, K., Strasser, P., Kawamura, N., Shimomura, K., Miyake, Y., Saito, T. and Higemoto, W. Development of Elemental Analysis by Muonic X-ray Measurement in J-PARC. *Journal of Physics: Conference Series*. IOP Publishing. 2010, vol. 225. 012040.

42. Higemoto, W., Kadono, R., Kawamura, N., Koda, A., Kojima, K. M., Makimura, S., Matoba, S., Miyake, Y., Shimomura, K. and Strasser, P. Materials and Life Science Experimental Facility at the Japan Proton Accelerator Research Complex IV: The Muon Facility. *Quantum Beam Science*, 2017. 1(1): 11.

43. Terada, K., Ninomiya, K., Osawa, T., Tachibana, S., Miyake, Y., Kubo, M., Kawamura, N., Higemoto, W., Tsuchiyama, A., Ebihara, M. *et al.* A New X-ray Fluorescence Spectroscopy for Extraterrestrial Materials using a Muon Beam. *Scientific Reports*, 2014. 4: 5072.

44. Zinatulina, D., Briançon, C., Brudanin, V., Egorov, V., Perevoshchikov, L., Shirchenko, M., Yutlandov, I. and Petitjean, C. Electronic Catalogue of Muonic X-rays. *EPJ Web of Conferences*. EDP Sciences. 2018, vol. 177. 03006.

45. Bowman, J., Poskanzer, A., Korteling, R. and Butler, G. Detection of Neutron-excess Isotopes of Low-Z Elements Produced in High-energy Nuclear Reactions. *Physical Review C*, 1974. 9(3): 836.

46. Byrne, A. R. Review of Neutron Activation Analysis in the Standardization and Study of Reference Materials, Including its Application to Radionuclide Reference Materials. *Fresenius' Journal of Analytical Chemistry*, 1993. 345(2-4): 144–151.

47. Blachot, J. Nuclear Data Sheets for A= 104. *Nuclear Data Sheets*, 2007. 108(10): 2035–2172.

48. De Frenne, D. Nuclear Data Sheets for A= 103. *Nuclear Data Sheets*, 2009. 110(9): 2081–2256.

49. De Frenne, D. Nuclear Data Sheets for A= 102. *Nuclear Data Sheets*, 2009. 110(8): 1745–1915.

50. Blachot, J. Nuclear Data Sheets update for A= 101. *Nuclear Data Sheets*, 1991. 63: 305–371.

51. Singh, B. and Chen, J. Nuclear Data Sheets for A= 100. *Nuclear Data Sheets*, 2021. 172: 1–542.

52. Browne, E. and Tuli, J. Nuclear Data Sheets for A=99. *Nuclear Data Sheets*, 2017. 145: 25–340.

53. Chen, J. and Singh, B. Nuclear Data Sheets for A= 98. *Nuclear Data Sheets*, 2020. 164: 1–477.

54. Nica, N. Nuclear data sheets for A= 97. *Nuclear Data Sheets*, 2010. 111(3): 525–716.

55. Abriola, D. and Sonzogni, A. Nuclear data sheets for A= 96. *Nuclear Data Sheets*, 2008. 109(11): 2501–2655.

56. Basu, S., Mukherjee, G. and Sonzogni, A. Nuclear data sheets for A= 95. *Nuclear Data Sheets*, 2010. 111(10-11): 2555–2737.

57. Abriola, D. and Sonzogni, A. Nuclear data sheets for A= 94. *Nuclear Data Sheets*, 2006. 107(9): 2423–2578.

58. Baglin, C. M. Nuclear data sheets for A= 93. *Nuclear Data Sheets*, 2011. 112(5): 1163–1389.

59. Baglin, C. M. Nuclear data sheets for A= 92. *Nuclear Data Sheets*, 2012. 113(10): 2187–2389.

60. Baglin, C. M. Nuclear data sheets for A= 91. *Nuclear Data Sheets*, 2013. 114(10): 1293–1495.

61. Basu, S. and Mccutchan, E. A. Nuclear Data Sheets for A= 90. *Nuclear Data Sheets*, 2020. 165: 1–329.

62. Sato, A., Kuno, Y., Sakamoto, H., Hino, Y., Tran, N., Truong, N., Cook, S., D'Arcy, R., Fukuda, M., Hatanaka, K. *et al.* Music, the world's Highest Intense DC Muon Beam using a Pion Capture System. *Proceedings of the 2nd International Particle Accelerator Conference (IPAC'11)*. 2011. 820–822.

63. Abela, R., Foroughi, F. and Renker, D. Muon Beams at PSI. *Zeitschrift für Physik C Particles and Fields*, 1992. 56(1): S240–S242.

64. Kammel, P., Collaborations, M. *et al.* Muon Capture and Muon Lifetime. *arXiv Preprint nucl-ex/0304019*, 2003.

65. Miyake, Y., Shimomura, K., Kawamura, N., Strasser, P., Koda, A., Makimura, S., Fujimori, H., Ikedo, Y., Nakahara, K., Takeshita, S. *et al.* J-PARC Muon Facility, MUSE. *Physics Procedia*, 2012. 30: 46–49.

66. Jacot-Guillarmod, R., Bienz, F., Boschung, M., Piller, C., Schaller, L., Schellenberg, L., Schneuwly, H., Reichart, W. and Torelli, G. Muon Transfer from Hydrogen to Argon and Helium at 10–15 Bars. *Physical Review A*, 1988. 38(12): 6151.

67. Measday, D. F., Stocki, T. J., Moftah, B. A. and Tam, H. γ Rays from Muon Capture in ^{27}Al and Natural Si. *Physical Review C*, 2007. 76(3): 035504.

68. Fynbo, H. O. U., Egorov, V., Brudanin, V., Chirtchenko, M., Deutsch, J., Lebedev, V., Petitjean, C., Riisager, K. and Vassiliev, S. The Muon Capture Rate of ^{48}Ca. *Nuclear Physics A*, 2003. 724(3-4): 493–501.

69. Sahu, A. K., Dash, D. K., Mishra, K., Mishra, S. P., Yadav, R. and Kashyap, P. Properties and Applications of Ruthenium. In: *Noble and Precious Metals-Properties, Nanoscale Effects and Applications*. IntechOpen. 2018.

70. Arnold, R., Augier, C., Barabash, A., Basharina-Freshville, A., Blondel, S., Blot, S., Bongrand, M., Brudanin, V., Busto, J., Caffrey, A. *et al.* Investigation of Double Beta Decay of ^{100}Mo to Excited States of ^{100}Ru. *Nuclear Physics A*, 2014. 925: 25–36.

71. Chan, K., Senin, H. and Naimah, I. Structural and Mechanical Properties of Polyvinyl Alcohol (pva) Thin Film. *AIP Conference Proceedings*. AIP. 2009, vol. 1136. 366–369.

72. Awada, H. and Daneault, C. Chemical Modification of Poly (vinyl alcohol) in Water. *Applied Sciences*, 2015. 5(4): 840–850.

73. Jayasekara, R., Harding, I., Bowater, I., Christie, G. and Lonergan, G. T. Preparation, Surface Modification and Characterisation of Solution Cast Starch PVA Blended Films. *Polymer Testing*, 2004. 23(1): 17–27.

74. Hamdalla, T. A. and Hanafy, T. A. Optical Properties Studies for PVA/Gd, La, Er or Y Chlorides Based on Structural Modification. *Optik-International Journal for Light and Electron Optics*, 2016. 127(2): 878–882.

75. Khatua, C., Chinya, I., Saha, D., Das, S., Sen, R. and Dhar, A. Modified Clad Optical Fibre Coated With PVA/TiO_2 Nano Composite For Humidity Sensing Application. *International Journal on Smart Sensing & Intelligent Systems*, 2015. 8(3).

76. Mbhele, Z., Salemane, M., Van Sittert, C., Nedeljković, J., Djoković, V. and Luyt, A. Fabrication and Characterization of Silver- polyvinyl Alcohol Nanocomposites. *Chemistry of Materials*, 2003. 15(26): 5019–5024.

77. Tiwari, A., Khan, S., Kher, R., Dhoble, S. and Chandel, A. Synthesis, Characterization and Optical Properties of Polymer-based ZnS Nanocomposites. *Luminescence*, 2016. 31(2): 428–432.

78. Zhang, Y., Yi, Z., Wei, L., Kong, L. and Wang, L. Modified Iron Phosphate/Polyvinyl Alcohol Composite Film for Controlled-release Fertilisers. *RSC Advances*, 2018. 8(32): 18146–18152.

79. Leo, W. R. *Techniques for Nuclear and Particle Physics Experiments: a How-to approach*. Springer Science & Business Media. 2012.

80. Takahashi, T., Awaya, Y., Tonuma, T., Kumagai, H., Izumo, K., Nishida, M., Hitachi, A., Hashizume, A., Uchiyama, S. and Doke, T. Stopping Power of Ni, Ag, Au, and Pb for 7-MeV/nucleon α Particles and Carbon ions: Z_3^1 deviation from the Bethe formula. *Physical Review A*, 1983. 27(3): 1360.

81. Norizan, M., Hashim, I., Ibrahim, F. and Ghani, N. Statistical Estimation of Ideal and Realistic Muon Interaction on Al, Fe, and Cu absorbers. *IOP Conference Series: Materials Science and Engineering*. IOP Publishing. 2020, vol. 785. 012006.

82. Akira, S. RCNP Experiment E. *Proposal for Experiment at RCNP: Muon-gamma Spectroscopy for Neutrino Nuclear Responses*, 2014.

83. Andert, K., Banifatov, A., Gansorig, D., Kalinin, A., Krogulski, T. and Zorin, G. Timing in Fission Fragment Detection at High Alpha-background. *Nuclear Instruments and Methods*, 1975. 129(2): 397–401.

84. Ganzorig, D., Hansen, P., Johansson, T., Jonson, B., Konijn, J., Krogulski, T., Kuznetsov, V., Polikanov, S., Tibell, G. and Westgaard, L. The Muon Capture Rate in ^{232}Th and ^{238}U Studied in the Fission Mode. *Physics Letters B*, 1978. 78(1): 41–43.

85. Borisov, S. and Podberezskaya, N. X-ray Diffraction Analysis: A Brief History and Achievements of the First Century. *Journal of Structural Chemistry*, 2012. 53(1).

86. Foelske, A., Barbieri, O., Hahn, M. and Kötz, R. An X-ray Photoelectron Spectroscopy Study of Hydrous Ruthenium Oxide Powders with Various Water Contents for Supercapacitors. *Electrochemical and Solid-state Letters*, 2006. 9(6): A268–A272.

87. Lenar, N., Paczosa-Bator, B. and Piech, R. Optimization of Ruthenium Dioxide Solid Contact in Ion-selective Electrodes. *Membranes*, 2020. 10(8): 182.

88. Sugimoto, W., Iwata, H., Yokoshima, K., Murakami, Y. and Takasu, Y. Proton and electron conductivity in hydrous ruthenium oxides evaluated by electrochemical impedance spectroscopy: the origin of large capacitance. *The Journal of Physical Chemistry B*, 2005. 109(15): 7330–7338.

89. Lee, J., Shah, S. A. S., Yoo, P. J. and Lim, B. Hydrous RuO2 nanoparticles as highly active electrocatalysts for hydrogen evolution reaction. *Chemical Physics Letters*, 2017. 673: 89–92.

90. Kannan, S. and Sundrarajan, M. Green Synthesis of Ruthenium Oxide Nanoparticles: Characterization and its Antibacterial Activity. *Advanced Powder Technology*, 2015. 26(6): 1505–1511.

91. Bunaciu, A. A., UdriŞTioiu, E. G. and Aboul-Enein, H. Y. X-ray diffraction: instrumentation and applications. *Critical reviews in analytical chemistry*, 2015. 45(4): 289–299.

92. Kumar, K. N., Padma, R., Rao, J. and Kang, M. Dazzling Green Emission from Graphene Oxide Nanosheet-embedded Co-doped Ce 3^{+} and Tb 3^{+}: PVA Polymer Nanocomposites for Photonic Applications. *RSC Advances*, 2016. 6(59): 54525–54538.

93. Siddaiah, T., Ojha, P., Kumar, N. O. and Ramu, C. Structural, optical and thermal characterizations of PVA/MAA: EA polyblend films. *Materials Research*, 2018. 21.

94. Lee, J., Lee, K. J. and Jang, J. Effect of silica nanofillers on isothermal crystallization of poly (vinyl alcohol): In-situ ATR-FTIR study. *Polymer testing*, 2008. 27(3): 360–367.

95. Ramírez-Hernández, A., Aguilar-Flores, C. and Aparicio-Saguilán, A. Fingerprint analysis of FTIR spectra of polymers containing vinyl acetate. *Dyna*, 2019. 86(209): 198–205.

96. Chen, L., Yuan, C., Gao, B., Chen, S. and Zhang, X. Microwave-assisted Synthesis of Organic–inorganic Poly (3, 4-ethylenedioxythiophene)/$RuO_2 \cdot {}_xH_2O$ Nanocomposite for Supercapacitor. *Journal of Solid State Electrochemistry*, 2009. 13(12): 1925.

97. Tsuji, E., Imanishi, A., Fukui, K.-i. and Nakato, Y. Electrocatalytic Activity of Amorphous RuO_2 Electrode for Oxygen Evolution in an Aqueous Solution. *Electrochimica Acta*, 2011. 56(5): 2009–2016.

98. Wu, Z.-S., Wang, D.-W., Ren, W., Zhao, J., Zhou, G., Li, F. and Cheng, H.-M. Anchoring Hydrous RuO_2 on Graphene Sheets for High-performance Electrochemical Capacitors. *Advanced Functional Materials*, 2010. 20(20): 3595–3602.

99. Kim, H. and Popov, B. N. Characterization of hydrous ruthenium oxide/carbon nanocomposite supercapacitors prepared by a colloidal method. *Journal of Power Sources*, 2002. 104(1): 52–61.

100. Korotcov, A. V., Huang, Y.-S., Tiong, K.-K. and Tsai, D.-S. Raman scattering characterization of well-aligned RuO2 and IrO2 nanocrystals. *Journal of Raman Spectroscopy: An International Journal for Original Work in all Aspects of Raman Spectroscopy, Including Higher Order Processes, and also Brillouin and Rayleigh Scattering*, 2007. 38(6): 737–749.

101. Chen, R., Chen, C., Huang, Y., Chia, C.-T., Chen, H., Tsai, D. and Tiong, K.-K. A comparative study of microstructure of RuO2 nanorods via Raman

scattering and field emission scanning electron microscopy. *Solid state communications*, 2004. 131(6): 349–353.

102. Neuffer, D., Bao, Y. and Hansen, G. Phase rotation of muon beams for producing intense low-energy muon beams. *arXiv preprint arXiv:1607.00028*, 2016.

103. Miyake, Y., Shimomura, K., Kawamura, N., Strasser, P., Makimura, S., Koda, A., Fujimori, H., Nakahara, K., Takeshita, S., Kobayashi, Y. *et al.* J-PARC Muon Facility, MUSE. *Journal of Physics: Conference Series*. IOP Publishing. 2010, vol. 225. 012036.

104. Statistical Calculation of Energy Loss Using Bethe-Bloch formula for muon Interaction with Aluminium, Iron and Copper, 2019. URL `http://sps.utm.my/wp-content/uploads/2018/08/Thesis-Preparation-05082018.pdf`.

105. Stratton, G. Comparison of a High Purity Germanium Gamma Ray Spectrometer and a Multidimensional NaI (T1) Scintillation Gamma Ray Spectrometer. 2011.

106. Akkurt, I., Tekin, H. and Mesbahi, A. Calculation of Detection Efficiency for the Gamma Detector Using MCNPX. *Acta Phys. Pol. A*, 2015. 128(2-B): 332–334.

107. Lépy, M.-C. Detection Efficiency. *Laboratoire National Henri Becquerel, CEA Saclay, F-91191 Gif-sur-Yvette cedex, France, IAEA-ALMERA Technical Visit*, 2010.

108. Pylypchynets, I., Lengyel, A., Parlag, O., Maslyuk, V. and Potoki, I. Empirical Formula for the HPGe-detector Efficiency Dependence on Energy and Distance. *Journal of Radioanalytical and Nuclear Chemistry*, 2019. 319(3): 1315–1319.

109. Energy Resolution in Gamma Spectrometry, 2016. URL `https://physicsopenlab.org/2016/02/07/energy-resolution-in-gamma-spectrometry/`.

110. Hino, Y., Kuno, Y., Sato, A., Sakamoto, H., Matsumoto, Y., Tran, N., Hashim, I., Fukuda, M., Hayashida, Y., Ogitsu, T., Yamamoto, A. and

Yoshida, M. A Highly intense DC muon source, MuSIC and muon CLFV search. *Nuclear Physics B - Proceedings Supplements*, 2014. 253-255: 206–207. ISSN 0920-5632. doi:https://doi.org/10.1016/j.nuclphysbps.2014.09.051. URL https://www.sciencedirect.com/science/article/pii/S0920563214001820, the Twelfth International Workshop on Tau-Lepton Physics (TAU2012).

111. RCNP-MuSIC Towards a New Era of Muon Science, 2015. URL http://www.rcnp.osaka-u.ac.jp/RCNPhome/music/facilities.html.

112. Katakam, L. N. and Aboul-Enein, H. Y. Elemental Impurities Determination by ICP-AES/ICP-MS: A review of Theory, Interpretation of Concentration Limits, Analytical Method Development Challenges and Validation Criterion for Pharmaceutical Dosage Forms. *Current Pharmaceutical Analysis*, 2020. 16(4): 392–403.

113. Porwal, N., Natarajan, V., Kumar, M., Rajeswari, B., Kulkarni, M., Bhide, M., Dhawale, B. and Godbole, S. EDXRF Determination of Dy, Eu, Gd and Sm in Aqueous Solutions. *Indian Journal of Chemistry*, 2010. 49A: 1052–1055.

114. Suoranta, T., Niemelä, M. and Perämäki, P. Comparison of Digestion Methods for the Determination of Ruthenium in Catalyst Materials. *Talanta*, 2014. 119: 425–429.

115. Laroche, G., Fitremann, J. and Gherardi, N. FTIR-ATR spectroscopy in thin film studies: The importance of sampling depth and deposition substrate. *Applied surface science*, 2013. 273: 632–637.

116. Amma, S.-i., Kim, S. H. and Pantano, C. G. Analysis of water and hydroxyl species in soda lime glass surfaces using attenuated total reflection (ATR)-IR spectroscopy. *Journal of the American Ceramic Society*, 2016. 99(1): 128–134.

117. Baran, Ö. *Determination of narcotic and psychotropic substances by using infrared spectroscopy*. Master's Thesis. Middle East Technical University. 2005.

118. Bumbrah, G. S. and Sharma, R. M. Raman spectroscopy–Basic principle, instrumentation and selected applications for the characterization of drugs of abuse. *Egyptian Journal of Forensic Sciences*, 2016. 6(3): 209–215.

119. Singh, S. B., Hu, Y., Kshetri, T., Kim, N. H. and Lee, J. H. An embedded-PVA@Ag nanofiber network for ultra-smooth, high performance transparent conducting electrodes. *J. Mater. Chem. C*, 2017. 5: 4198–4205.

120. Restrepo, I., Medina, C., Meruane, V., Akbari-Fakhrabadi, A., Flores, P. and Rodríguez-Llamazares, S. The effect of molecular weight and hydrolysis degree of poly (vinyl alcohol)(PVA) on the thermal and mechanical properties of poly (lactic acid)/PVA blends. *Polímeros*, 2018. 28: 169–177.

121. Zhang, R., Xu, W. and Jiang, F. Fabrication and characterization of dense chitosan/polyvinyl-alcohol/poly-lactic-acid blend membranes. *Fibers and Polymers*, 2012. 13(5): 571–575.

122. Ye, H., Yu, T., Li, Y., Zhang, Y., Xin, Q., Zhao, L. and Li, H. Manipulation of Grafting Location via Photografting To Fabricate High-Performance Ethylene Vinyl Alcohol Copolymer Membrane for Protein Separation. *ACS omega*, 2019. 4(2): 3514–3526.

123. Povinec, P. *Rare Nuclear Processes-Proceedings Of The 14th Eps Nuclear Physics Conference*. World Scientific. 1992.

124. Bhaskar, S., Dobal, P., Majumder, S. and Katiyar, R. X-ray photoelectron spectroscopy and micro-Raman analysis of conductive RuO 2 thin films. *Journal of Applied Physics*, 2001. 89(5): 2987–2992.

125. Yahmadi, B., Kamoun, N., Guasch, C. and Bennaceur, R. Synthesis and characterization of nanocrystallized In2S3 thin films via CBD technique. *Materials Chemistry and Physics*, 2011. 127(1-2): 239–247.

126. Sivayoganathan, M., Tan, B. and Venkatakrishnan, K. Synthesis of Crystalline and Amorphous, Particle-agglomerated 3-D Nanostructures of Al and Si Oxides by Femtosecond Laser and the Prediction of these Particle Sizes. *Nanoscale Research Letters*, 2012. 7(1): 1–7.

127. Deshmukh, P., Pusawale, S., Bulakhe, R. and Lokhande, C. Supercapacitive Performance of Hydrous Ruthenium Oxide ($RuO_2 \cdot nH_2O$) Thin films

Synthesized by Chemical Route at Low Temperature. *Bulletin of Materials Science*, 2013. 36(7): 1171–1176.

128. Mink, J., Kristof, J., De Battisti, A., Daolio, S. and Németh, C. Investigation on the Formation of RuO_2-based Mixed Oxide Coatings by Spectroscopic methods. *Surface science*, 1995. 335: 252–257.

129. Kim, J. and Lin, Y. Synthesis and Characterization of Suspension-Derived, Porous Ion-Conducting Ceramic Membranes. *Journal of the American Ceramic Society*, 1999. 82(10): 2641–2646.

130. Mesoroentgen Spectra Catalogue, 2003. URL `http://muxrays.jinr.ru/about.html`.

131. Firestone, R. Table of Isotopes 8th Edition Vol. 1, 1996.

132. Nuclear Data Table, 2021. URL `https://www.nndc.bnl.gov/nudat2/chartNuc.jsp`.

133. Hashim, I., Ejiri, H., Othman, F., Saroni, S., Amelia, W., Hamzah, S. and Wei, K. Statistical neutron emission model for neutrino nuclear response. *EPJ Web of Conferences*. EDP Sciences. 2017, vol. 156. 00005.

134. Tomono, D., Fukuda, M., Hatanaka, K., Higemoto, W., Ieiri, M., Kawashima, Y., Kuno, Y., Matsuzaki, T., Minakawa, M., Miyake, Y., Nakazawa, Y., Ninomiya, K., Mori, Y., Morinobu, S., Satod, A., Shimomura, K., Takahisa, K., Taniguchi, A., Weichao, Y. and L. Wong, M. Construction of new DC muon beamline, MuSIC-RCNP, for muon applied science. *PoS*, 2018. NuFact2017: 111. doi:10.22323/1.295.0111.

LIST OF PUBLICATIONS

Journal with Impact Factor

1. Hashim, I.H., Ejiri, H., Othman, F., Ibrahim, F., Soberi, F., Ghani, N.N.A.M.A., Shima, T., Sato, A. and Ninomiya, K., 2020. Nuclear Isotope Production by Ordinary Muon Capture Reaction. *Nuclear Instruments and Methods in Physics Research Section A: Accelerators, Spectrometers, Detectors and Associated Equipment*, p.163749. https://doi.org/10.1016/j.nima.2020.163749. **(Q1, IF:1.265)**

Indexed Journal (SCOPUS)

1. Norizan, M. I. H. M., Hashim, I. H., Ibrahim, F., and Ghani, N. N. A. M. A. (2020, April). Statistical Estimation of ideal and realistic muon interaction on Al, Fe, and Cu absorbers. *IOP Conference Series: Materials Science and Engineering*, 785(1), p.012006. https://doi.org/10.1088/1757-899X/785/1/012006
2. Ghani, N. N. A., Saeed, M. A., and Hashim, I. H. (2017). Thermoluminescence (TL) response of silica nanoparticles subjected to 50 Gy gamma irradiation. *Malays Journal Fundamental Applied Science*, 13(3), 178-180. https://doi.org/10.11113/mjfas.v13n3.593

Indexed conference proceedings

1. Nik Noor Aien Mohamed Abdul Ghani, Izyan Hazwani Hashim, Muhammad Firdaus Omar, and Yung Szen Yap. (2020). Analysis of the Physical and Elemental Properties of RuO_2 Thin Film. *Proceeding of the XX International Symposium on Solid State Dosimetry 2020*, 1, 64-77.